



**HAL**  
open science

## A global event with a regional character: the Early Toarcian Oceanic Anoxic Event in the Pindos Ocean (northern Peloponnese, Greece)

N. Kafousia, V. Karakitsios, H.C Jenkyns, Emanuela Mattioli

► **To cite this version:**

N. Kafousia, V. Karakitsios, H.C Jenkyns, Emanuela Mattioli. A global event with a regional character: the Early Toarcian Oceanic Anoxic Event in the Pindos Ocean (northern Peloponnese, Greece). *Geological Magazine*, 2011, 148 (4), pp.619-631. 10.1017/S0016756811000082 . hal-00661408

**HAL Id: hal-00661408**

**<https://hal.science/hal-00661408>**

Submitted on 19 Jul 2012

**HAL** is a multi-disciplinary open access archive for the deposit and dissemination of scientific research documents, whether they are published or not. The documents may come from teaching and research institutions in France or abroad, or from public or private research centers.

L'archive ouverte pluridisciplinaire **HAL**, est destinée au dépôt et à la diffusion de documents scientifiques de niveau recherche, publiés ou non, émanant des établissements d'enseignement et de recherche français ou étrangers, des laboratoires publics ou privés.

# A global event with a regional character: the Early Toarcian Oceanic Anoxic Event in the Pindos Ocean (northern Peloponnese, Greece)

N. KAFOUSIA\*†, V. KARAKITSIOS\*, H. C. JENKYNST‡ & E. MATTIOLIS§

\*Department of Geology and Geoenvironment, National University of Athens, Panepistimiopolis, 15784 Athens, Greece

‡Department of Earth Sciences, University of Oxford, South Parks Road, Oxford OX1 3AN, UK

§Université Claude Bernard Lyon I, UMR 5125, CNRS, PaléoEnvironnements et PaléobioSphère, Département des Sciences de la Terre, 2 rue Dubois, 69622 Villeurbanne, France

(Received 3 March 2010; accepted 3 December 2010)

**Abstract** – The Early Toarcian (Early Jurassic, *c.* 183 Ma) was characterized by an Oceanic Anoxic Event (T-OAE), primarily identified by the presence of globally distributed approximately coeval black organic-rich shales. This event corresponded with relatively high marine temperatures, mass extinction, and both positive and negative carbon-isotope excursions. Because most studies of the T-OAE have taken place in northern European and Tethyan palaeogeographic domains, there is considerable controversy as to the regional or global character of this event. Here, we present the first high-resolution integrated chemostratigraphic (carbonate, organic carbon,  $\delta^{13}\text{C}_{\text{carb}}$ ,  $\delta^{13}\text{C}_{\text{org}}$ ) and biostratigraphic (calcareous nannofossil) records from the Kastelli Pelites cropping out in the Pindos Zone, western Greece. During the Mesozoic, the Pindos Zone was a deep-sea ocean-margin basin, which formed in mid-Triassic times along the northeast passive margin of Apulia. In two sections through the Kastelli Pelites, the chemostratigraphic and biostratigraphic (nannofossil) signatures of the most organic-rich facies are identified as correlative with the Lower Toarcian, *tenuicostatum/polymorphum-falciferum/serpentinum/levisoni* ammonite zones, indicating that these sediments record the T-OAE. Both sections also display the characteristic negative carbon-isotope excursion in organic matter and carbonate. This occurrence reinforces the global significance of the Early Toarcian Oceanic Anoxic Event.

Keywords: Toarcian Oceanic Anoxic Event, Pindos Zone, carbon isotopes, Greece, Kastelli Pelites.

## 1. Introduction

The Early Toarcian (*c.* 183 Ma) was associated with global warming (Bailey *et al.* 2003; Jenkyns, 2003), mass extinction (Little & Benton, 1995; Wignall, Newton & Little, 2005) and a globally increased rate of organic carbon burial attributed to an Oceanic Anoxic Event (OAE) (Jenkyns, 1985, 1988, 2010; Karakitsios, 1995; Rigakis & Karakitsios, 1998; Jenkyns, Gröcke & Hesselbo, 2001; Karakitsios *et al.* 2004, 2007). The Toarcian OAE (T-OAE) coincides with an overall positive and interposed negative carbon-isotope excursion that has been recorded in marine organic matter, pelagic and shallow-water marine carbonates, brachiopods and fossil wood (Hesselbo *et al.* 2000, 2007; Schouten *et al.* 2000; Röhl *et al.* 2001; Kemp *et al.* 2005; van Breugel *et al.* 2006; Suan *et al.* 2008, 2010; Woodfine *et al.* 2008; Hermoso *et al.* 2009; Sabatino *et al.* 2009). To date, most research has concentrated on N European and Tethyan palaeogeographic environments, representing shelf seas and drowned carbonate platforms on foundered continental margins (Bernoulli & Jenkyns, 1974, 2009). Thus, an ongoing vigorous debate exists as to whether the recorded patterns of Toarcian carbon burial and carbon-isotope evolution represent only

processes occurring within these relatively restricted palaeogeographic marine environments or whether they were truly global in character (e.g. Küspert, 1982; van der Schootbrugge *et al.* 2005; Wignall *et al.* 2006; Hesselbo *et al.* 2007; Svensen *et al.* 2007; Suan *et al.* 2008). Those pointing to local factors suggest overturning of a stratified water column rich in CO<sub>2</sub> from the oxidation of organic matter; those suggesting global control suggest introduction of isotopically light carbon into the ocean–atmosphere system from dissociation of gas hydrates or hydrothermal venting of greenhouse gases. Certainly, the recent recognition of the T-OAE in Argentina suggests the impact of this phenomenon was not confined to the northern hemisphere (Al-Suwaidi *et al.* 2010).

In Greece, only limited geochemical data are available for the T-OAE (Jenkyns, 1988). During the period from the Triassic to the Late Cretaceous, the external Hellenides (western Greece) constituted part of the southern Tethyan margin (Fig. 1), where siliceous and organic carbon-rich sediments were commonly associated facies (Bernoulli & Renz, 1970; Karakitsios, 1995; de Wever & Baudin, 1996). The Ionian and Pindos zones of western Greece (Fig. 2) expose such basinal, thrust-imbricated sediments that document continental (Ionian Zone) and continent–ocean-margin basinal pelagic sequences (Pindos Zone).

†Author for correspondence: nkafousia@geol.uoa.gr

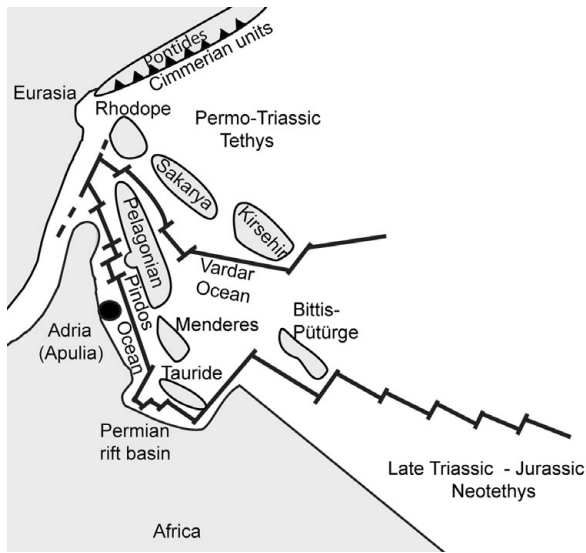


Figure 1. Early Jurassic palaeogeography of the western Tethys Ocean (based on Clift, 1992; Dercourt, Ricou & Vrielynck, 1993; Channell & Kozur, 1997; Degnan & Robertson, 1998; Pe-Piper, 1998). The approximate position of the study area is illustrated by the black circle. The stable segment of Adria is approximately the size of the area now occupied by the Adriatic Sea, parts of eastern Italy, the Southern Alps and Istria.

of the Kastelli Pelites, here unambiguously identified as deposited during the Early Toarcian OAE, strongly reinforce the global character of the T-OAE.

**2. Geological setting and stratigraphy**

The Pindos Zone (Fig. 2) exposes an imbricate thrust belt with allochthonous Mesozoic to Tertiary sedimentary rocks of deep-water facies. The zone extends into Albania and former Yugoslavia (Dédé *et al.* 1976; Robertson & Karamata, 1994) as well as into Crete (Bonneau, 1984), Rhodes (Aubouin *et al.* 1976) and Turkey (Bernoulli, de Graciansky & Monod, 1974; Argyriadis *et al.* 1980). The sediments of the Pindos Zone originate from an elongate remnant ocean basin that formed in mid-Triassic time along the northeastern passive margin of Apulia between the extensive Gavrovo–Tripolis platform in the present west and the Pelagonian continental block in the east (including also the isolated Parnassos Platform in its western portion). Continental collision in the Aegean area has produced a collage of microcontinental blocks, which were accreted to the active margin of Eurasia in early Tertiary times. Observations on the Greek mainland as well as on the island of Crete confirm that the eastern basal rocks of the Pindos Zone and the southwestern end of the Pelagonian continental terrane were rifted from Gondwana in mid-Triassic times (De Wever, 1976; Bonneau, 1982; Clift, 1992; Degnan & Robertson, 1998; Pe-Piper, 1998). By Early Jurassic

In this study, we present for the first time a high-resolution isotopic record of the T-OAE in Tethyan ocean-margin sediments, deposited in an area corresponding to the western edge of the Pindos Ocean. Integrated chemostratigraphic and biostratigraphic studies

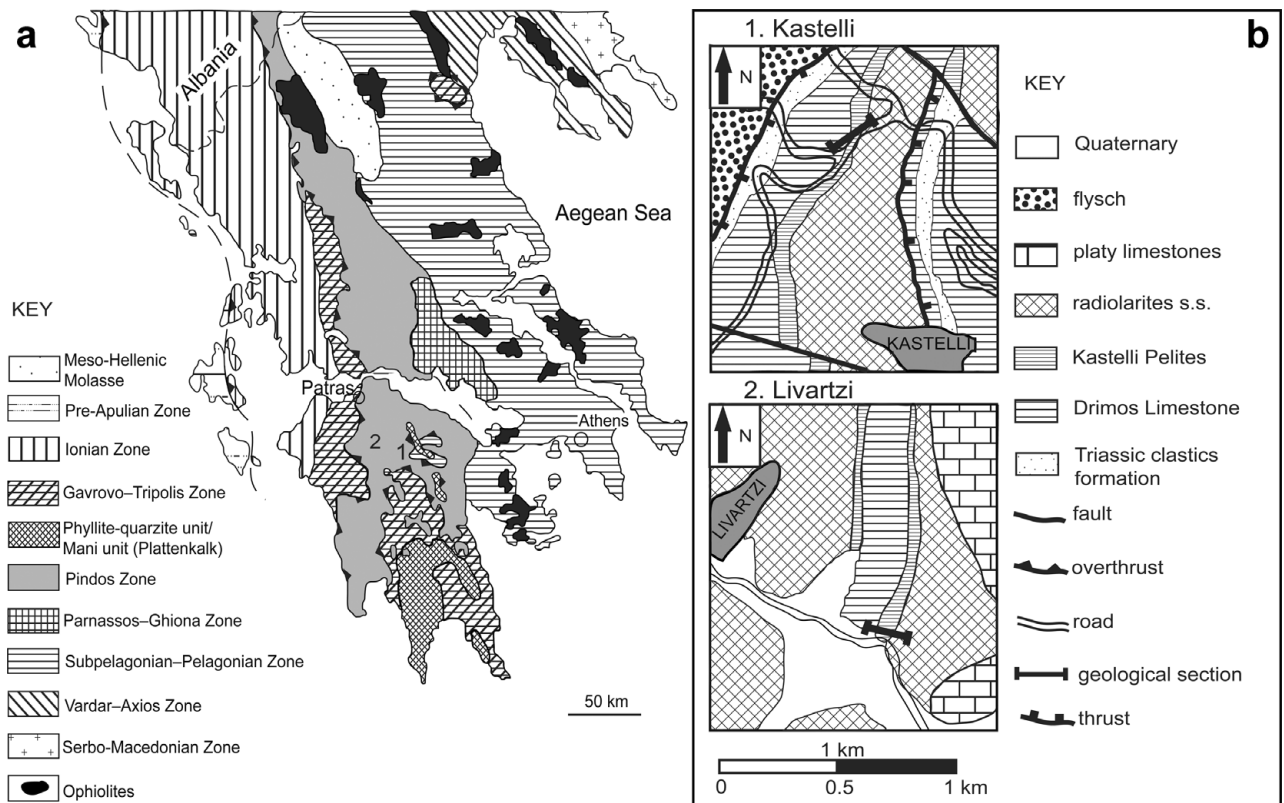


Figure 2. (a) Simplified geological map with the main tectonostratigraphic zones of the Hellenides. (b) Geological map of Kastelli section (above) and Livartzi section (below).

time at the latest (Fig. 1), actively spreading oceanic basins had opened in both the Pindos and the Vardar Zones on either side of the Pelagonian continental block (De Wever, 1976; Bonneau, 1982; Robertson *et al.* 1991; Clift, 1992; Lefèvre *et al.* 1993; Pe-Piper & Hatzipanagiotou, 1993; Degnan & Robertson, 1998; Pe-Piper, 1998). The evidence indicating the oceanic character of the Pindos Basin is summarized by Degnan & Robertson (1998). The western Pindos Ocean separated Pelagonia from Apulia; the eastern Vardar Ocean separated Pelagonia from the Serbomacedonia and Sarakya microcontinents. Later Mesozoic and Cenozoic convergence resulted in the nappe structure of the Hellenide Orogen and the tectonic dismemberment of the Permian–Triassic rift-related igneous rocks. The amount of orogen-parallel transport during closure of the Pindos and Vardar oceans is uncertain, but most authors argue that it was not large (Robertson *et al.* 1991; Wooller, Smith & White, 1992). The Pindos Zone of western Greece is exceptional since it was deformed into a regular series of thrust sheets during its emplacement, with a minimum of disruption. The present-day westward-vergent fold and thrust sheets have not been affected by major back-thrusting or out-of-sequence thrusting (Degnan & Robertson, 1998).

The sedimentary successions of the Pindos Zone comprise deep-water carbonate, siliciclastic and siliceous rocks, ranging in age from Late Triassic to Eocene (Fleury, 1980; Degnan & Robertson, 1998).

### 3. Field observations

#### 3.a. Kastelli section

The Kastelli section (37° 54' N, 22° 02' E) is located about 200 m westwards of the junction of the Kalavrita–Klitoria and Kalavrita–Aroania roads. In this section, the outcrop is of excellent quality and illustrates, in stratigraphic continuity, the Drimos Limestone Formation, the Kastelli Pelites and the radiolarites *sensu stricto*. The outcrops correspond to the eastern more distal part of the Pindos western margin. From the bottom to top the following lithological units are observed:

(i) The Drimos Limestone Formation, which comprises sediments some 100 m thick. The lower part is 35 m thick and is developed as an alternation of limestones, with filaments (thin-shelled bivalves), and green pelites. This unit, which is chert-bearing, is dated as Norian, at a point about 300 m southwest of this section (J. M. Flament, unpub. Ph.D. thesis, Univ. Lille, 1973). A radiolarian cherty member, about 10 m thick, divides the lower from the upper part, which comprises mainly limestones attaining some 60 m in thickness. A precise age determination in this upper part is not possible with the observed faunas, because they are represented only by some reworked algae and Foraminifera (e.g. *Thaumatoporella* sp. and *Textulariida*, respectively).

(ii) The Kastelli Pelites, comprising sediments about 35 m thick. The first 8 m consists of a succession of thin-layered (5–10 cm) marly limestones alternating with mainly grey marls (a limestone layer with chert nodules is interbedded in the lower part of the succession). The sequence continues with 3–4 m of red marls, marly clays and clays with some intercalations of marly limestone. Above, there follows some 6 m of mainly marly limestones and marls containing rare black chert layers. In thin-sections of the marly limestones, badly preserved Foraminifera are observed. The succession finishes with 5 m of marly limestones and red marls, cherty at the top. These cherts indicate a passage into the stratigraphically overlying radiolarites *sensu stricto*.

#### 3.b. Livartzi section

The Livartzi section (37° 55' N, 21° 55' E) is located north of the Tripotama–Kalavrita road by the turning towards Livartzi village. The outcrop corresponds to the western (closer to the Tripolis Platform) part of the Pindos margin. Here the Kastelli Pelites are thinner (20 m thick) than those of the Kastelli section itself (35 m thick).

The sampling started in the upper 6 m of the Drimos Limestone Formation, comprising thin layers of marly limestone. Quaternary sediments cover the first 3 m of Kastelli Pelites. After this exposure gap, there follows a 1 m marly limestone bed, and the section continues with the typical Kastelli Pelites Formation, as described for the type locality.

### 4. Methods

In total, 325 bulk sediment samples were collected from the two sections (191 from Kastelli and 134 from Livartzi). The collected samples were powdered and analysed for weight per cent total organic carbon and the equivalent amount of CaCO<sub>3</sub> using a Strohlein Coulomat 702 analyser (details in Jenkyns, 1988), for carbonate carbon and oxygen isotopes using a VG Isogas Prism II mass spectrometer (details in Jenkyns, Gale & Corfield, 1994) and for organic-matter carbon and oxygen isotopes using a Europa Scientific Limited CN biological sample converter connected to a 20–20 stable-isotope gas-ratio mass spectrometer (details in Jenkyns *et al.* 2007). All the above analyses were undertaken in the Department of Earth Sciences and Research Laboratory for Archaeology in the University of Oxford. Results for both sections are given in Tables A1 and A2 in the online Appendix at <http://journals.cambridge.org/geo>.

A set of 27 samples from Kastelli and 28 from Livartzi was investigated for its content of calcareous nannofossils. Smear-slides were prepared from the powdered rock according to the technique described in Bown & Young (1998), then analysed in an optical polarizing Leitz microscope at × 1250. Nannofossils

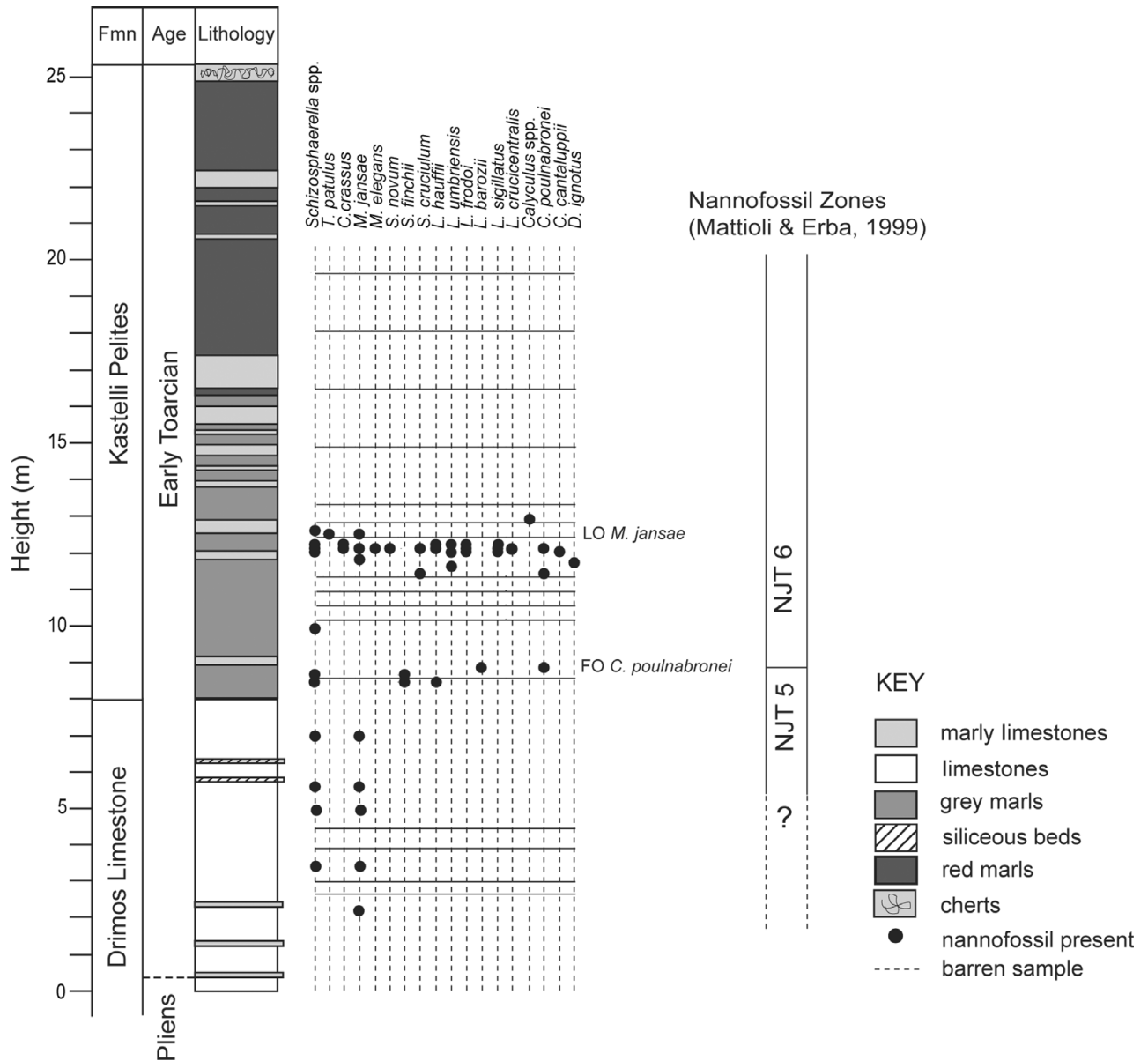


Figure 3. Lithological column and biostratigraphical data from the Kastelli section. Nannofossil zones after Mattioli & Erba (1999).

222 were counted for each sample in a surface area of the  
 223 slide varying between 1 and 2 cm<sup>2</sup>.

224 **5. Results**

225 **5.a. Biostratigraphy**

226 There are very few data concerning the age of the  
 227 Kastelli Pelites, the lack of ammonites indicating that  
 228 the sequence was deposited below the aragonite com-  
 229 pensation depth. Lyberis, Chotin & Doubinger (1980)  
 230 attributed the unit to the Late Pliensbachian/Toarcian,  
 231 comparing the palynological associations with those  
 232 of the Vicentin Alps. Nevertheless, the only precise  
 233 data are referred to by Fleury (1980) and de Wever  
 234 & Origlia-Devos (1982), who suggest an Aalenian  
 235 age for the top of the Kastelli Pelites unit. Fleury's  
 236 (1980) data are based on the presence of *Meyendorffina*  
 237 (*Lucasella*) *cayeuxi* (Lucas) in a limestone layer at

the top of Kastelli Pelites in the Karpenission region 238  
 (central Greece); and de Wever & Origlia-Devos's 239  
 (1982) data are based on Foraminifera faunas from 240  
 the Peloponnese. Based on general biostratigraphic 241  
 and chemostratigraphic considerations, Jenkyns (1988) 242  
 suggested that the Kastelli Pelites were correlative with 243  
 other black shales in Greece (in the Ionian Zone) and 244  
 were formed during the T-OAE. 245

We undertook detailed biostratigraphical analyses of 246  
 calcareous nannofossils in an effort to improve and 247  
 expand the biostratigraphical resolution from previous 248  
 studies. The nannofossil distribution is summarized in 249  
 Figures 3 and 4. 250

251 *5.a.1. Kastelli section*

Samples were taken from the limestones at the top 252  
 of the Drimos Limestone Formation, as well as from 253  
 the lower to middle part of the Kastelli Pelites for 254

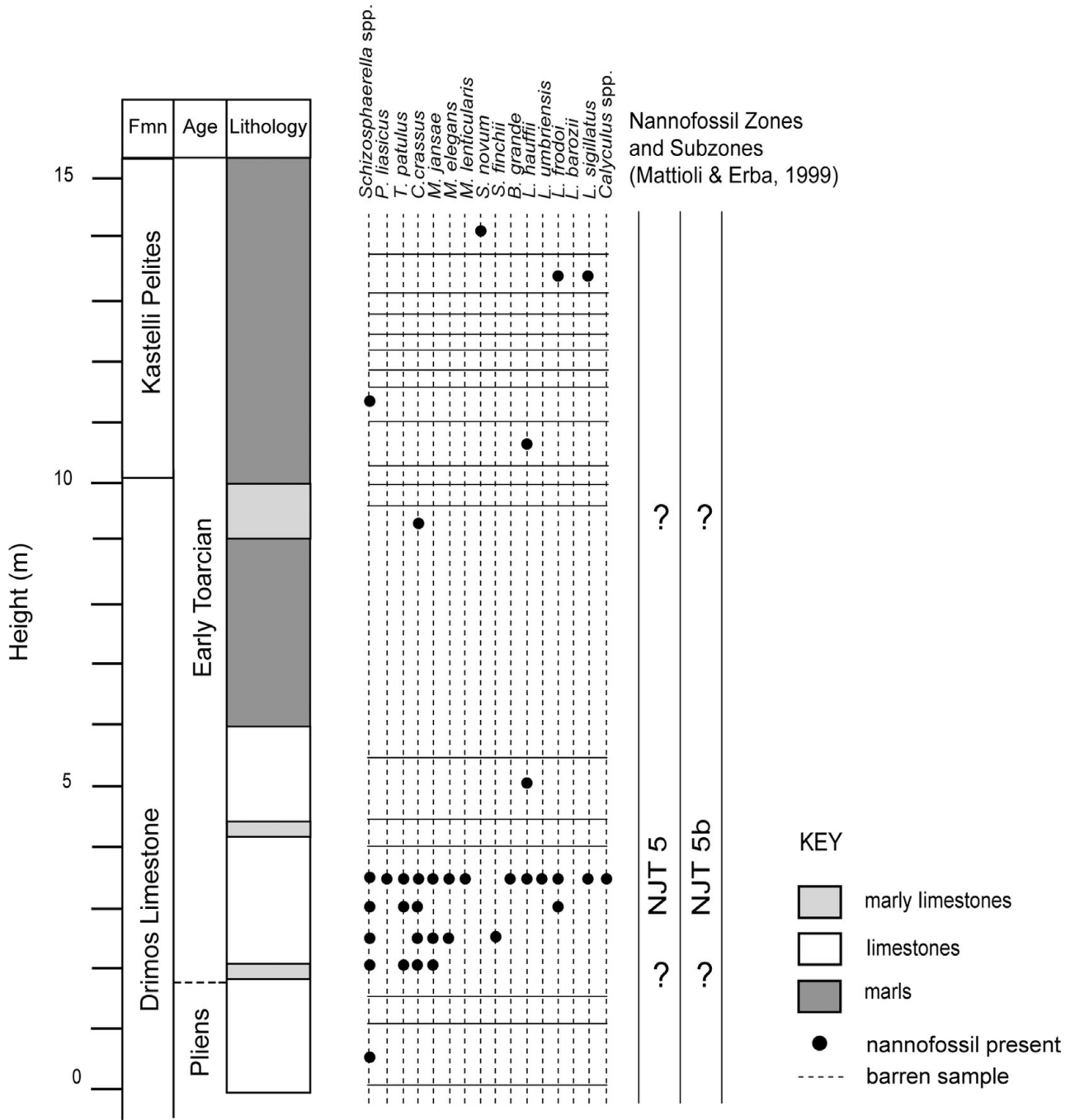


Figure 4. Lithological column and biostratigraphical data from the Livartzi section. Nannofossil zones after Mattioli & Erba (1999).

255 a thickness of about 20 m. Twelve samples were  
 256 barren of nannofossils, and the rest contained very  
 257 few specimens. The assemblage is represented by rare  
 258 *Schizosphaerella* spp., *Mitrolithus jansae* and *M. elegans*,  
 259 *Calyculus* spp., *Similiscutum cruciulum*, *S. finchii*  
 260 and *S. novum*, *Tubirhabdus patulus*, *Crepidolithus*  
 261 *crassus*, and various species of the genus *Lotharingius*,  
 262 including the zonal marker *L. hauffii*. This assemblage  
 263 allows us to identify the NJT 5 nannofossil Zone (Late  
 264 Pliensbachian to Early Toarcian). Specimens belonging  
 265 to the *Carinolithus* genus, namely *C. poulabronei*  
 266 and *C. cantaluppii*, were recorded discontinuously  
 267 starting from sample 34. This occurrence can be used  
 268 at Kastelli to identify the NJT 6 nannofossil Zone. The

last occurrence of *Mitrolithus jansae* was observed in  
 sample 71 (12.5 m). A single specimen of *Discorhab-*  
*odus ignotus* was encountered in sample 63 (12 m). The  
 first occurrence of this species is fixed at the *tenu-*  
*icostatum/serpentinum* zonal boundary in central Italy  
 (Mattioli & Erba, 1999), where it is considered to mark  
 the end of the Early Toarcian OAE (Bucefalo Palliani &  
 Mattioli, 1998; Mattioli *et al.* 2004), although in some  
 areas an earlier occurrence of *D. ignotus* is recorded  
 (Mattioli *et al.* 2008; Bodin *et al.* 2010).

5.a.2. Livartzi section

Only 14 samples of the Livartzi section were found  
 to contain calcareous nannofossils. The productive

269  
 270  
 271  
 272  
 273  
 274  
 275  
 276  
 277  
 278  
 279  
 280  
 281

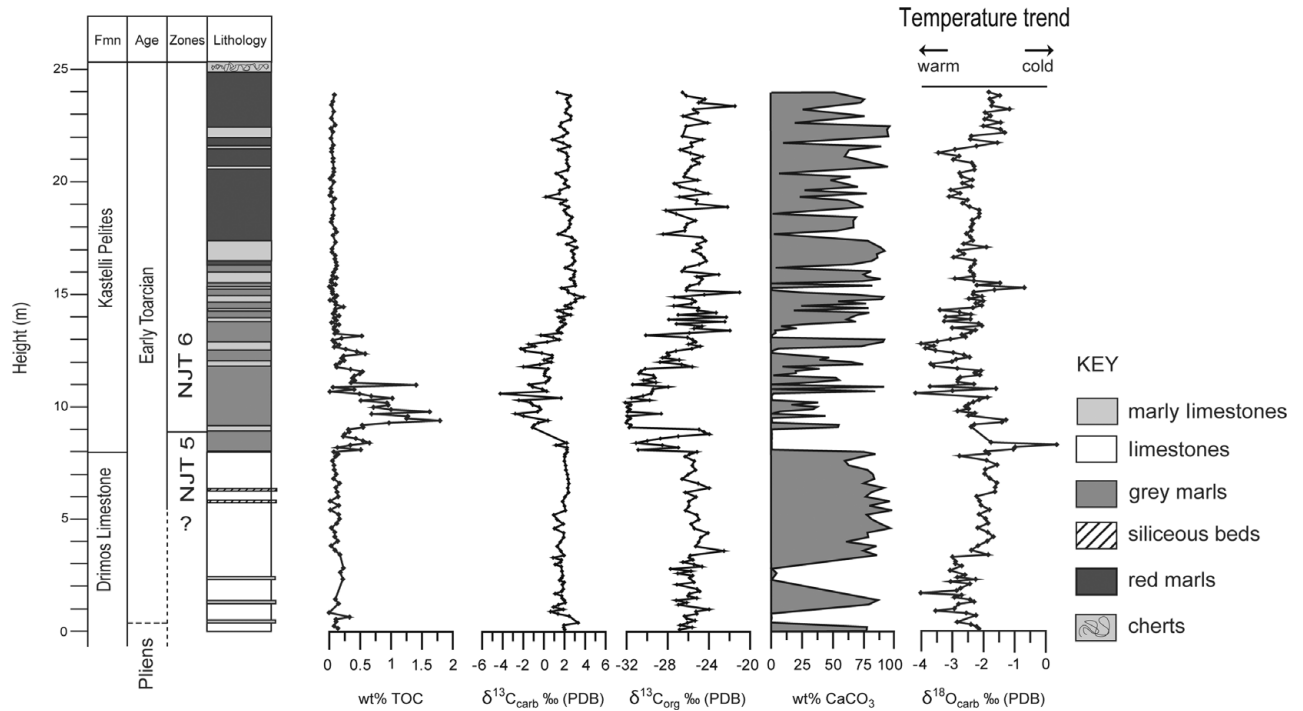


Figure 5. Lithostratigraphical log, bulk TOC, stable-isotope (C, O) and wt % CaCO<sub>3</sub> profiles through the Kastelli section. For a colour version of this figure see online Appendix at <http://journals.cambridge.org/geo>.

282 samples show assemblages similar to those of the  
 283 Kastelli section with poorly preserved and rare nano-  
 284 fossils. The interval between samples 11 and 36  
 285 (from 1.1 to 3.6 m) represents an exception, because  
 286 samples are richer, with common *Schizosphaerella* and  
 287 *M. jansae*. The stratigraphically highest specimen of  
 288 *M. jansae* is recorded in sample 36 (3.6 m). However,  
 289 we cannot confidently define this datum level as  
 290 a last occurrence because the samples studied in  
 291 the interval above are barren of nannofossils. This  
 292 assemblage, and the presence in the assemblage of *L.*  
 293 *sigillatus*, allows attribution of this interval to the NJT  
 294 5b nannofossil Subzone (uppermost Pliensbachian to  
 295 lowermost Toarcian).

## 296 5.b. Chemostratigraphy

### 297 5.b.1. Kastelli section

298 5.b.1.a. Organic carbon and carbonate profiles Chemo-  
 299 stratigraphic data are illustrated in Figure 5. The  
 300 total organic carbon (TOC) values are very low and  
 301 stable in the lower part of the section where back-  
 302 ground values are in the range 0.10–0.20 wt %. After the lowest  
 303 7.5 m, the TOC values begin to rise gradually for 1.5 m  
 304 defining a positive excursion to reach a maximum value  
 305 of 1.79 wt %. At the top of this interval, values return  
 306 to background levels.

307 The carbonate values do not follow any particular  
 308 trend nor do they respond to the excursion. Up to the  
 309 level where the TOC excursion begins, the percentage  
 310 of CaCO<sub>3</sub> in the bulk rock fluctuates between 60 and  
 311 100 %. When the excursion begins, there is a sudden  
 312 drop to reach values lower than 10 %; following that,

313 values start to rise again until the top of the studied  
 314 section, with relative minima being attained every few  
 315 metres. A similar pattern is seen in other Tethyan  
 316 pelagic sections recording the T-OAE (e.g. Sabatino  
 317 *et al.* 2009).

### 318 5.b.1.b. Stable-isotope (carbon and oxygen) profiles

319 The carbon- and oxygen-isotope values in carbonate  
 320 and the TOC of bulk rock are reported in Figure 5. The  
 321 bulk carbonate carbon-isotope values record a small  
 322 positive followed by a negative excursion in the lowest  
 323 metre of the section. Above this small disturbance, val-  
 324 ues are very stable within the next 7.5 m of the section,  
 325 with background values of 2 ‰. Thereafter,  $\delta^{13}\text{C}_{\text{carb}}$   
 326 values begin to fall irregularly, reaching a minimum of  
 327  $-5$  ‰. The negative excursion extends over the  
 328 next 5 m before recovery takes place and back-  
 329 ground values of  $\sim 2$  ‰ are restored. What is remarkable is  
 330 the polarity between the TOC profile and the carbonate  
 331 carbon-isotope profile, with the two curves appearing as  
 332 approximate mirror images of one another. The strati-  
 333 graphical coincidence between the negative carbon-  
 334 isotope excursion and relative TOC maximum is also  
 335 observed in Toarcian black shales from northwestern  
 336 Europe and central Italy (Jenkyns & Clayton, 1997;  
 337 Jenkyns *et al.* 2002; Mattioli *et al.* 2004).

338 The organic carbon-isotope profile is slightly differ-  
 339 ent from that of  $\delta^{13}\text{C}_{\text{carb}}$ . The first shift is recorded in  
 340 the interval 8 to 9 m and records a drop from  $-25.15$  ‰  
 341 to  $-31.1$  ‰; following this excursion, values return  
 342 to  $-24.95$  ‰. Above this level, values drop again, to  
 343  $-32.1$  ‰, and remain low for approximately 2.5 m.  
 344 Stratigraphically higher in the section, values become

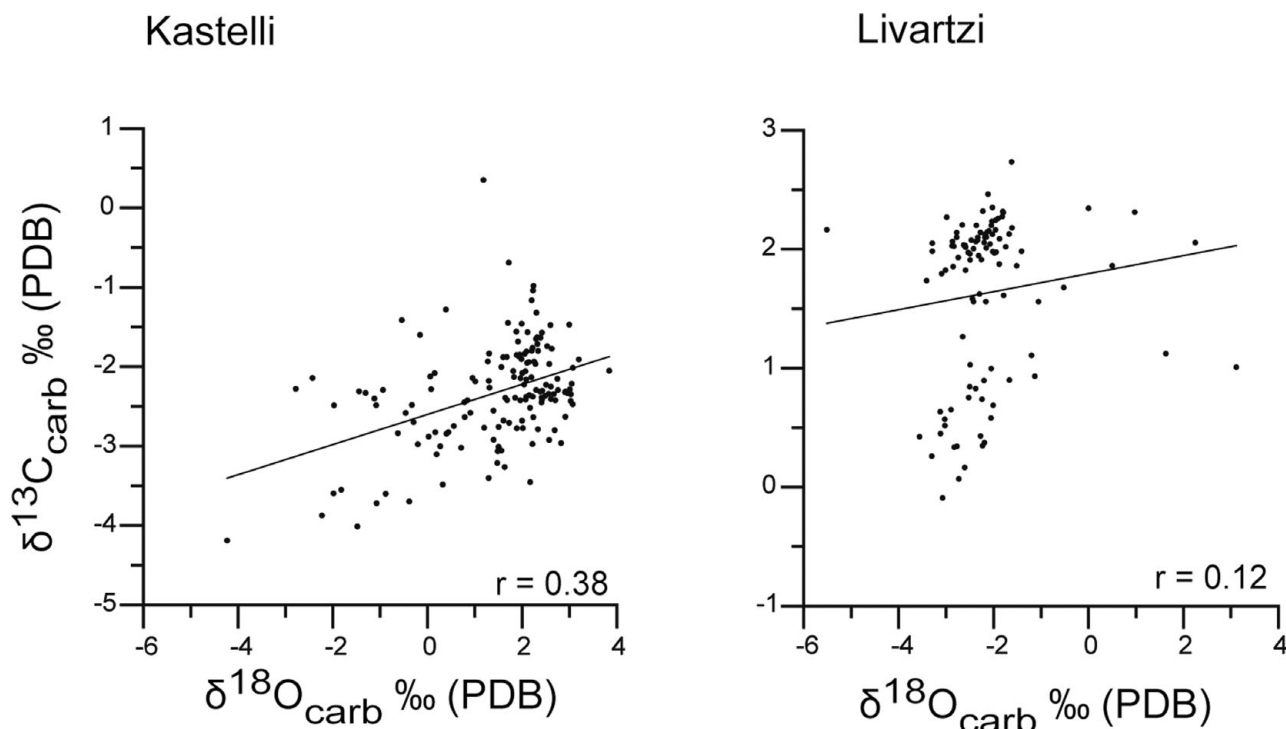


Figure 6. Cross-plot of  $\delta^{13}\text{C}_{\text{carb}}$  and  $\delta^{18}\text{O}_{\text{carb}}$  data from the Kastelli and Livartzi sections. For a colour version of this figure see online Appendix at <http://journals.cambridge.org/geo>.

heavier and fluctuate around a background value of  $-25\text{‰}$ .

Oxygen-isotope values are generally in the range of  $-2\text{‰}$  (Fig. 5), which is a typical value for  $\delta^{18}\text{O}$  in Tethyan Pliensbachian/Toarcian boundary carbonates, boreal belemnites and brachiopods (Jenkyns & Clayton, 1986; McArthur *et al.* 2000; Jenkyns *et al.* 2002; Rosales, Robles & Quesada, 2004; Suan *et al.* 2008). At the 8.5 m level of the section, there is a positive spike of about  $2\text{‰}$ , above which there is a shift towards lighter values. The lighter values correspond stratigraphically to the negative excursion of the carbon isotopes.  $\delta^{18}\text{O}$  values remain low and do not return to  $-2\text{‰}$  until the 21.5 m level of the section. To what extent these carbonates record primary palaeotemperature signals and to what extent they have been modified by diagenesis is not known, but some primary signature is assumed, given the correlation with palaeotemperature trends established elsewhere in Europe (Bailey *et al.* 2003; Jenkyns, 2003). The cross-plot of  $\delta^{13}\text{C}_{\text{carb}}$  and  $\delta^{18}\text{O}_{\text{carb}}$  values (Fig. 6) gives a Pearson's correlation coefficient value  $r$  of 0.38, which implies moderate correlation between oxygen- and carbon-isotopic values. If it is assumed that an increase in temperature (lowering  $\delta^{18}\text{O}$  values) would follow from an introduction of isotopically light carbon in the ocean-atmosphere system (as  $\text{CH}_4$  or  $\text{CO}_2$ ), some correlation between  $\delta^{18}\text{O}$  and  $\delta^{13}\text{C}$  would be expected (e.g. Jenkyns, 2003).

#### 5.b.2. Livartzi section

**5.b.2.a. Organic carbon and carbonate profiles** The TOC values and the percentage of  $\text{CaCO}_3$  in bulk rock

are reported in Figure 7. In this section, the TOC values are even lower than those at Kastelli, ranging from undetectable to 0.6 wt %. Nevertheless, an interval of relatively high values is located between the 9.6 and 11.2 m levels. Above and below that interval, TOC values are close to zero. The  $\text{CaCO}_3$  content of the section is in general relatively high ( $> 70\%$ ), except for levels higher than that of the TOC maximum, where  $\text{CaCO}_3$  values drop to less than 10 %.

#### 5.b.2.b. Stable-isotope (carbon and oxygen) profiles

The carbonate carbon-isotope and the organic carbon-isotope stratigraphy of the Livartzi section are shown in Figure 7. This section has two distinct negative excursions. The  $\delta^{13}\text{C}_{\text{carb}}$  in the Drimos Limestone Formation is very stable and constant at  $\sim 2\text{‰}$ . Above the 3 m sampling gap, values drop until they reach a minimum of  $-0.09\text{‰}$ , then remain low for  $\sim 1.5$  m. Thereafter follows the second negative excursion that extends over a greater thickness of section ( $\sim 2$  m) but only drops to  $0.45\text{‰}$ . Towards the top of the section,  $\delta^{13}\text{C}_{\text{carb}}$  values become higher.

The organic carbon-isotope profile approximately tracks the carbonate carbon-isotope profile, although there are differences. The  $\delta^{13}\text{C}_{\text{org}}$  signal in the limestones of the lower part of the section shows scattered data points, probably because only isotopically variable refractory carbon is present, given the very low TOC values. Stratigraphically higher, just after the gap, the isotopic values are low, reaching the minimum value of  $-31.85\text{‰}$ . The values remain low for  $\sim 1.5$  m. Higher in the section there is an increase of  $8.5\text{‰}$ , above which values begin to fall again through the rest of

377  
378  
379  
380  
381  
382  
383  
384  
385

386  
387  
388  
389  
390  
391  
392  
393  
394  
395  
396  
397

398  
399  
400  
401  
402  
403  
404  
405  
406  
407  
408

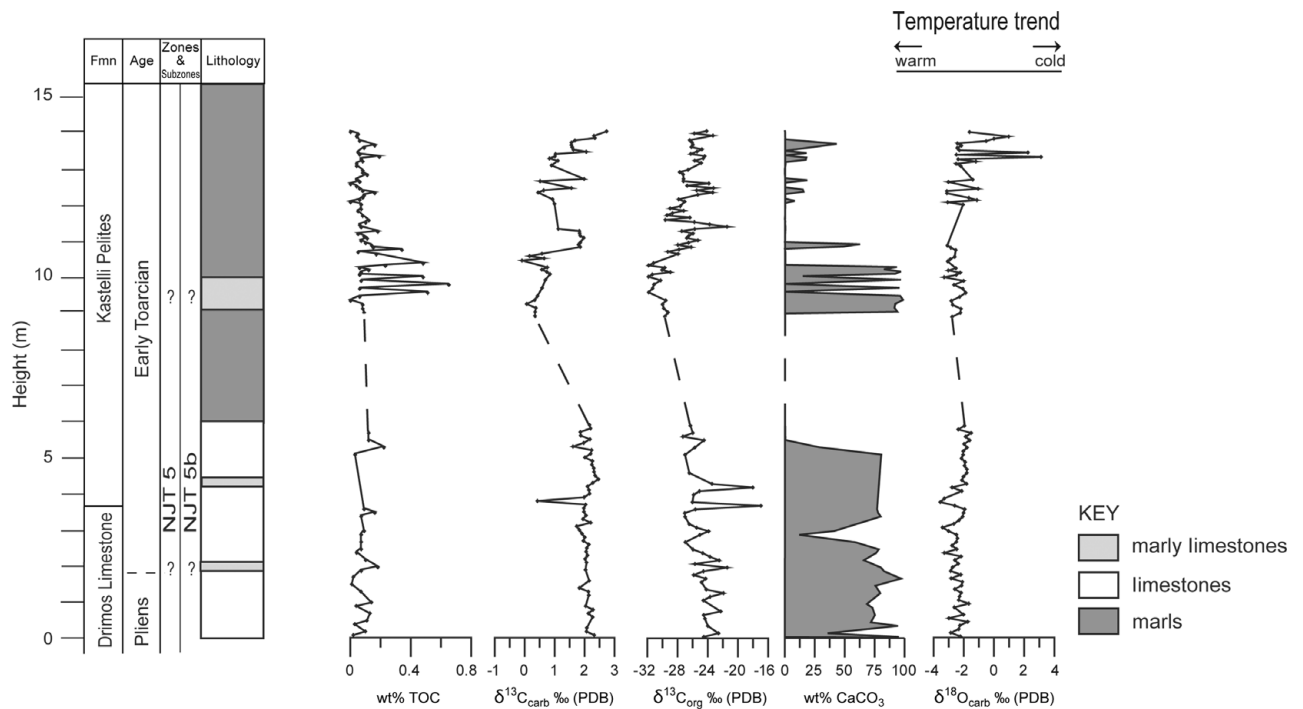


Figure 7. Lithostratigraphical log, bulk TOC, stable-isotope (C, O) and wt % CaCO<sub>3</sub> profiles through the Livartzi section. The dashed line represents a sampling gap. For a colour version of this figure see online Appendix at <http://journals.cambridge.org/geo>.

409 the section. In the upper part of the section the  $\delta^{13}\text{C}_{\text{org}}$   
410 values fluctuate around  $-25\text{‰}$ .

411 Oxygen-isotope values fluctuate in this section also  
412 around  $-2\text{‰}$  (Fig. 7). There is a small negative  
413 spike of about  $1\text{‰}$  at the level of the first carbon-  
414 isotope negative excursion. Higher in the section,  
415 around the level of the second carbon-isotope negative  
416 excursion, the  $\delta^{18}\text{O}$  values become heavier, reaching  
417 values up to  $\sim 4\text{‰}$ . The latter values are relatively  
418 high in comparison with other Tethyan Toarcian  
419 values. Moreover, as shown in Figure 6, the Pearson's  
420 correlation coefficient value of  $\delta^{13}\text{C}_{\text{carb}}$  and  $\delta^{18}\text{O}_{\text{carb}}$   
421 from this section is 0.12, which corresponds to a  
422 low degree of correlation between the isotopic values.  
423 Given the considerable difference between this and the  
424 Kastelli section, it is apparent that the  $\delta^{18}\text{O}$  values  
425 have been modified by diagenesis and do not record  
426 a primary isotopic record.

## 427 6. Discussion

### 428 6.a. New biostratigraphic data based 429 on calcareous nannofossils

430 In spite of the paucity of calcareous nannofossil  
431 assemblages recorded in the two studied sections,  
432 some significant biostratigraphic results are presented  
433 in this work that allow direct dating of the  
434 carbon-isotope curves from Kastelli and Livartzi in  
435 addition to correlation with biostratigraphically well-  
436 dated  $\delta^{13}\text{C}$  records from elsewhere. Although the  
437 standard chronostratigraphy of the Jurassic is based  
438 upon ammonite biostratigraphy, an increasing number  
439 of works present effective correlation of the Early

Toarcian negative isotope excursion (CIE) across the  
western Tethys based upon the ranges of calcareous  
nannofossils (Bucefalo Palliani, Mattioli & Riding,  
2002; Mattioli *et al.* 2004, 2008; Tremolada, van de  
Schootbrugge & Erba, 2005; Mailliot *et al.* 2006,  
2007; Bodin *et al.* 2010). In fact, the recognition of  
the NJT 6 nannofossil Zone in the Kastelli section  
allows unambiguous referral of the main negative CIE  
recorded in the Pindos Zone to the Early Toarcian  
and allows correlation with comparable phenomena  
associated with the Early Toarcian OAE in other NW  
European areas (Tremolada, van de Schootbrugge &  
Erba, 2005; Mattioli *et al.* 2008) as well as a section in  
N Africa (Bodin *et al.* 2010).

454 A preceding negative excursion of  $2\text{‰}$  below the  
455 main carbon-isotope excursion has been recorded  
456 in Peniche (Portugal) and constitutes a chemostrati-  
457 graphic marker for the Pliensbachian/Toarcian bound-  
458 ary (Hesselbo *et al.* 2007). In the Kastelli section, the  
459 carbonate carbon-isotope profile starts with a positive  
460 excursion of  $\sim 1\text{‰}$ , and follows with a negative excu-  
461 sion of the same range. This negative excursion is not  
462 clearly dated by calcareous nannofossils in the Kastelli  
463 section, but it lies just below an interval assigned to the  
464 NJT 5 Zone, spanning the Late Pliensbachian–Early  
465 Toarcian interval. This negative excursion resembles  
466 those also observed at the stage boundary in Yorkshire  
467 (NE England), Valdorbria, (Marche–Umbria, Italy) and  
468 the High Atlas of Morocco, as recorded by Sabatino  
469 *et al.* (2009), Littler, Hesselbo & Jenkyns (2010) and  
470 Bodin *et al.* (2010). Given the occurrence of this feature  
471 in the Pindos Zone, this isotopic feature, as proposed  
472 by Hesselbo *et al.* (2007) as at least a regional marker,  
473 is likely be of global significance.

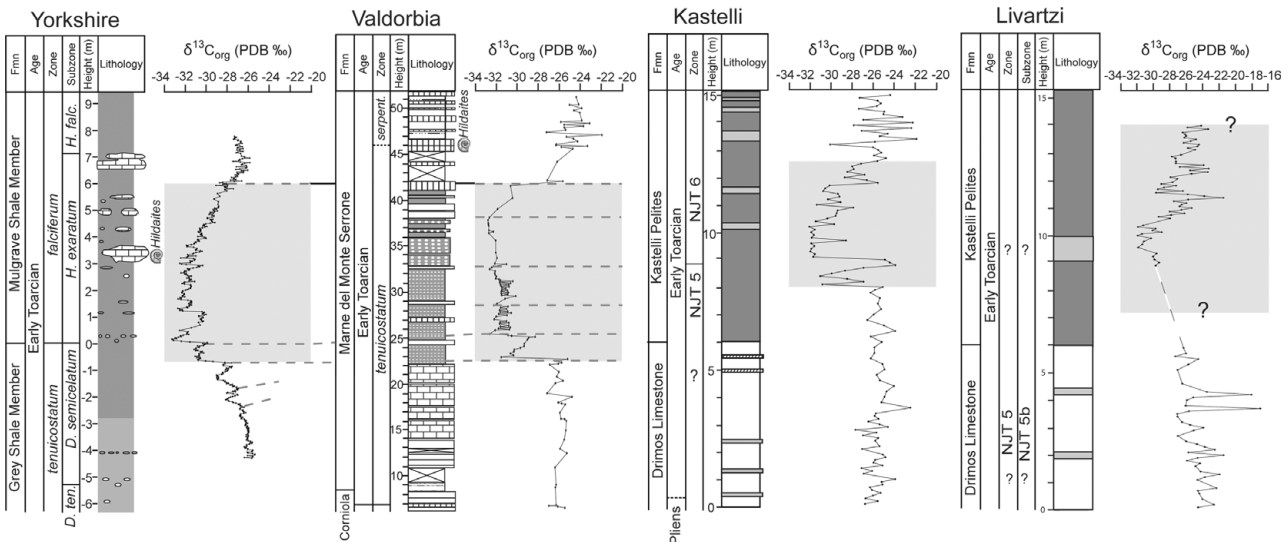


Figure 8. Comparison between the  $\delta^{13}C_{org}$  data from Yorkshire, UK (Kemp *et al.* 2005), Valdorbria, Italy (Sabatino *et al.* 2009), and Kastelli and Livartzi, Greece. For a colour version of this figure see online Appendix at <http://journals.cambridge.org/geo>.

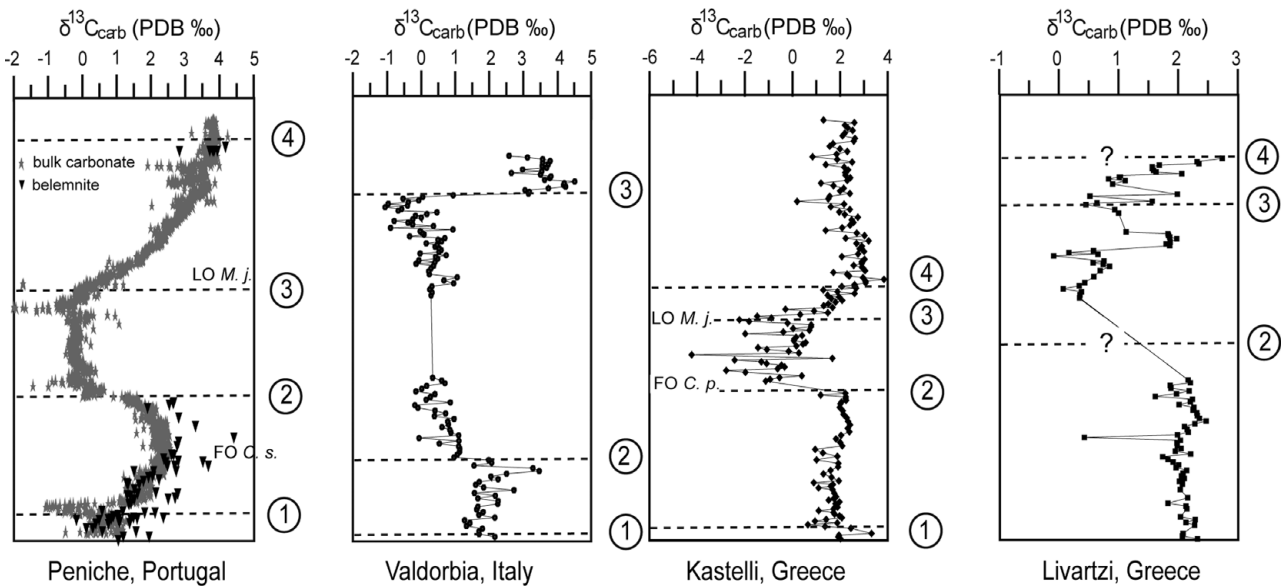


Figure 9. Comparison between the  $\delta^{13}C_{carb}$  data from Peniche, Portugal (Hesselbo *et al.* 2007), Valdorbria, Italy (Sabatino *et al.* 2009), and Kastelli and Livartzi, Greece. For a colour version of this figure see online Appendix at <http://journals.cambridge.org/geo>.

**6.b. The preservation of the organic matter**

In both stratigraphic sections, the TOC content is very low, especially in Livartzi, where it does not exceed 1%. TOC values in the Toarcian black shales of northern Europe are much higher, rising to ~15%, probably because of relatively elevated organic productivity, a high degree of water mass stratification, local euxinic conditions and lesser water depth (Jenkyns *et al.* 2002; Sabatino *et al.* 2009; Jenkyns, 2010). The palaeodepth of the Pindos Ocean was probably greater than that of typical Tethyan continental margins, as preserved in the Alps and the Apennines, and certainly greater than the epicontinental seas of northern Europe. With greater palaeodepths, organic matter would have had a greater transit distance and transit time to the sea floor, thus increasing the chance of oxidation before burial.

**6.c. European correlation of the carbon-isotope record and implications for the regional character of the OAE**

Suggested chemostratigraphic correlations between the Greek sections in the Pindos Zone and other extensively studied sections in Europe are illustrated in Figures 8 and 9. In Figure 8, the correlation is based mostly on the  $\delta^{13}C_{org}$  data from Yorkshire, Valdorbria, Kastelli and Livartzi, whereas in Figure 9, correlation is based mostly on the  $\delta^{13}C_{carb}$  data from Peniche, Valdorbria, Kastelli and Livartzi, using the four ‘key’ levels described by Hesselbo *et al.* (2007).

In Figure 8, the grey band and the dashed lines in the Yorkshire and Valdorbria profiles are based on  $\delta^{13}C_{org}$  data and their spectral analyses, whereas the comparison between these two sections and the Greek sections is based only on the shape of the

474  
475  
476  
477  
478  
479  
480  
481  
482  
483  
484  
485  
486  
487  
488  
489

490  
491  
492  
493  
494  
495  
496  
497  
498  
499  
500  
501  
502  
503  
504  
505

carbon-isotope excursion. In all four compared sections, the negative carbon-isotope excursion has a similar range of values, but each profile differs in detail. The Greek sections have a relatively small negative excursion in  $\delta^{13}\text{C}_{\text{org}}$  of  $\sim -5\%$ , after which values return to background values ( $\sim -25\%$ ). The grey band in the Greek sections marks the extent of the negative carbon-isotope excursion, which covers most, but not all, of the OAE interval, as defined in Yorkshire (Jenkyns, 2010). A suggested correlation between the Kastelli, Valdorbja and Peniche sections (Fig. 9) includes the Pliensbachian/Toarcian excursion (Level 1). Level 1 is not recognizable in the Livartzi section.

In both the Kastelli and Livartzi sections, the positive shift that is marked in Peniche directly above Level 1 is subdued. Level 2 is marked in all sections by the beginning of the negative carbon-isotope excursion. In Peniche, Level 2 is located at the *polymorphum*–*levisoni* zonal boundary and occurs above the first occurrence (FO) of the nanofossil *Carinolithus superbis* and *Carinolithus poul nabronei* (Mailliot *et al.* 2007). The nanofossil zone of *C. superbis* (referred to as NJT 6) has been suggested to coincide with the OAE (Mattioli *et al.* 2004). In the Kastelli section, the FO of *C. poul nabronei*, whose first occurrence is stratigraphically very close to that of *C. superbis* (Mattioli & Erba, 1999; Mailliot *et al.* 2007), is located in Level 2, although the lack of carbonate in adjacent parts of the section introduces some stratigraphic uncertainty. Neither the beginning of the negative carbon-isotope excursion nor the NJT 6 Zone is apparent in the Livartzi section; we therefore can only place Level 2 approximately at this location.

Level 3 in Peniche and Valdorbja is where  $\delta^{13}\text{C}_{\text{carb}}$  values reach a minimum and thereafter begin to increase. In Peniche, this level corresponds also to the TOC maximum (Hesselbo *et al.* 2007) whereas, in the other three sections, TOC values have already reached background values at this level. In Peniche, the last occurrence (LO) of *Mitrolithus jansae* is marked slightly above Level 3 (Mattioli *et al.* 2008), whereas in Kastelli, it corresponds to Level 3. The top of the section in Peniche is marked as Level 4 and it correlates with the end of the negative excursion and this can also be identified in the Kastelli section, although it is less clear-cut in the Livartzi section.

Although there is some minor diachroneity in nanofossil first and last occurrence datum levels with respect to the  $\delta^{13}\text{C}$  record, a striking correlation is documented in this study between the different isotope levels occurring across the negative carbon-isotope excursion in the Kastelli Pelites and other, more fossiliferous ammonite-bearing sections, underscoring the widespread nature of the event (Jenkyns *et al.* 1985, 2002; Jenkyns & Clayton, 1986, 1997; Mattioli *et al.* 2008; Sabatino *et al.* 2009).

## 7. Conclusions

Integrated chemostratigraphy and biostratigraphy confirm for the first time the age of the Kastelli Pelites of the Pindos Zone in Greece. They were formed during the Early Toarcian OAE and belong to the NJT 6 nanofossil Zone, correlative with the *tenuicostatum*–*falciferum* zones of northern Europe or its equivalents in southern Europe (*tenuicostatum/polymorphum*–*falciferum/serpentinum/levisoni* zones). The record of the T-OAE from these deep-marine sediments, which were part of the Tethyan Ocean, strongly supports the postulated global character of the T-OAE. The stratigraphic distribution of nanofossils and the shape of the negative carbon-isotope excursion differ from some different European sections, suggesting a degree of regional environmental control and/or diagenetic effects. The carbon-isotope profile from Kastelli resembles that of Valdorbja, Marche–Umbria, Italy (Sabatino *et al.* 2009), whereas that from Livartzi resembles that of Yorkshire, NE England (Kemp *et al.* 2005). The small negative excursion in carbon isotopes recently recorded at the Pliensbachian/Toarcian boundary in Peniche, Portugal, in Valdorbja, Italy, the High Atlas of Morocco and in Yorkshire, England, is also identified in the type section of the Kastelli Pelites.

**Acknowledgements.** The authors would like to thank Dr Norman Charnley (Earth Sciences Department) and Dr Peter Ditchfield (Archaeological Research Laboratory) for isotope analyses performed during a visit of NK to Oxford University. NK would like to thank the European Association of Organic Geochemists for the travel scholarship which she received, and University of Athens SARG for co-funding the field work. EM warmly thanks Mrs Paula Desvignes for help in smear-slide preparation. The reviewers are also thanked for their helpful comments.

## References

- AL-SUWAIDI, A. H., ANGELOZZI, G. N., BAUDIN, F., DAMBORENEA, S. E., HESSELBO, S. P., JENKYN, H. C., MANCENIDO, M. O., & RICCARDI, A. C. 2010. First record of the Early Toarcian Oceanic Anoxic Event from the Southern Hemisphere, Neuquén Basin, Argentina. *Journal of the Geological Society, London* **167**, 633–6.
- ARGYRIADIS, I., DE GRACIANSKY, P. C., MARCOUX, J. & RICO, L. E. 1980. The opening of the Mesozoic Tethys between Eurasia and Arabia-Africa. In *Géologie des chaînes alpines issues de la Téthys* (eds J. Aubouin, J. Debelmas & M. Latreille), pp. 199–214. 26th International Geological Congress, Paris, Colloque C5. *Bureau de Recherches Géologiques et Minières Mémoire*, **115**.
- AUBOUIN, J., BONNEAU, M., DAVIDSON, G. J., LÉBOULENGER, P., MATESKO, S. & ZAMBETAKIS, A. 1976. Esquisse structurale de l'Arc égéen externe: des Dinarides aux Taurides. *Bulletin de la Société géologique de France*, 7e série **18**, 327–36.
- BAILEY, T. R., ROSENTHAL, Y., MCARTHUR, J. M. & VAN DE SCHOOTBRUGGE, B. 2003. Paleooceanographic changes of the Late Pliensbachian-Early Toarcian interval: a possible link to the genesis of an Oceanic Anoxic Event. *Earth and Planetary Science Letters* **212**, 307–20.

- 626 BERNOULLI, D., De GRACIANSKY, P. C. D. & MONOD, O. 1974. The extension of the Lycian Nappes (SW Turkey) into the Southeastern Aegean Islands. *Eclogae Geologicae Helveticae* **67**, 39–90.
- 627  
628  
629  
630 BERNOULLI, D. & JENKYN, H. C. 1974. Alpine, Mediterranean and central Atlantic Mesozoic facies in relation to the early evolution of the Tethys. In *Modern and Ancient Geosynclinal Sedimentation* (eds R. H. Dott Jr. & R. H. Shaver), pp. 129–60. Society of Economic Paleontologists and Mineralogists, Special Publication 19.
- 631  
632  
633  
634  
635  
636  
637 BERNOULLI, D. & JENKYN, H. C. 2009. Ancient oceans and continental margins of the Alpine-Mediterranean Tethys: deciphering clues from Mesozoic pelagic sediments and ophiolites. *Sedimentology* **56**, 149–90.
- 638  
639  
640  
641  
642 BERNOULLI, D. & RENZ, O. 1970. Jurassic carbonate facies and new ammonite faunas from western Greece. *Eclogae Geologicae Helveticae* **65**, 573–607.
- 643  
644  
645 BODIN, S., MATTIOLI, E., FRÖHLICH, S., MARSHALL, J. D., BOUTIB, L., LAHSINI, S. & REDFERN, J. 2010. Toarcian carbon isotope shifts and nutrient changes from the Northern margin of Gondwana (High Atlas, Morocco, Jurassic): palaeoenvironmental implications. *Palaeogeography, Palaeoclimatology, Palaeoecology* **297**, doi: 10.1016/j.palaeo.2010.08.018, 377–390
- 646  
647  
648  
649  
650  
651  
652 BONNEAU, M. 1982. Evolution géodynamique de l'Arc égéen depuis le Jurassique supérieur jusqu'au Miocène. *Bulletin de la Société géologique de France, 7e série* **24**, 229–42.
- 653  
654  
655  
656  
657  
658  
659  
660  
661  
662  
663  
664  
665  
666  
667  
668  
669  
670  
671  
672  
673  
674  
675  
676  
677  
678  
679  
680  
681  
682  
683  
684  
685  
686  
687  
688  
689  
690  
691  
692  
693
- DÉDÉ, S., CILI, P., BUSHI, E. & MAKBUL, Y. 1976. Traits fondamentaux de la tectonique de Cukal. *Permbledhje Studimesh* **20/4**, 15–33.
- 694  
695  
696  
697  
698  
699  
700  
701  
702  
703  
704  
705  
706  
707  
708  
709  
710  
711  
712  
713  
714  
715  
716  
717  
718  
719  
720  
721  
722  
723  
724  
725  
726  
727  
728  
729  
730  
731  
732  
733  
734  
735  
736  
737  
738  
739  
740  
741  
742  
743  
744  
745  
746  
747  
748  
749  
750  
751  
752  
753  
754  
755  
756  
757  
758  
759  
760  
761
- DEGNAN, P. J. & ROBERTSON, A. H. F. 1998. Mesozoic–early Tertiary passive margin evolution of the Pindos Ocean (NW Peloponnese, Greece). *Sedimentary Geology* **117**, 33–70.
- DERCOURT, J., RICOU, L. E. & VRIELLYNCK, B. (eds) 1993. *Atlas Tethys Palaeoenvironmental Maps*. Paris: Gauthier-Villars, 307 pp.
- FLEURY, J. J. 1980. Les zones de Gavrovo-Tripolitza et du Pinde-Olonos (Grèce continentale et Péloponnèse du nord). Evolution d'une plate-forme et d'un bassin dans leur cadre alpin. *Société Géologique du Nord, Publication* **4**, 1–473.
- HERMOSO, M., Le CALLONEC, L., MINOLATTI, F., RENARD, M. & HESSELBO, S. P. 2009. Expression of the Early Toarcian negative carbon-isotope excursion in separated carbonate microfractions (Jurassic, Paris Basin). *Earth and Planetary Science Letters* **277**, 194–203.
- HESSELBO, S. P., GRÖCKE, D. R., JENKYN, H. C., BJERRUM, C. J., FARRIMOND, P., MORGANS BELL, H. S. & GREEN, O. R. 2000. Massive dissociation of gas hydrate during a Jurassic oceanic anoxic event. *Nature* **406**, 392–5.
- HESSELBO, S. P., JENKYN, H. C., DUARTE, L. V. & OLIVEIRA, L. C. V. 2007. Carbon-isotope record of the Early Jurassic (Toarcian) Oceanic Anoxic Event from fossil wood and marine carbonate (Lusitanian Basin, Portugal). *Earth and Planetary Science Letters* **253**, 455–70.
- JENKYN, H. C. 1985. The Early Toarcian and Cenomanian–Turonian anoxic events in Europe: comparisons and contrasts. *Geologische Rundschau* **74**, 505–18.
- JENKYN, H. C. 1988. The early Toarcian (Jurassic) anoxic event: stratigraphic, sedimentary, and geochemical evidence. *American Journal of Science* **288**, 101–51.
- JENKYN, H. C. 2003. Evidence for rapid climate change in the Mesozoic–Palaeogene greenhouse world. *Philosophical Transactions of the Royal Society London, Series A* **361**, 1885–916.
- JENKYN, H. C. 2010. The geochemistry of Oceanic Anoxic Events. *Geochemistry, Geophysics, Geosystems* **11**, Q03004, doi:10.1029/2009GC002788, 30 pp.
- JENKYN, H. C. & CLAYTON, C. J. 1986. Black shales and carbon isotopes in pelagic sediments from the Tethyan Lower Jurassic. *Sedimentology* **33**, 87–106.
- JENKYN, H. C. & CLAYTON, C. J. 1997. Lower Jurassic epicontinental carbonates and mudstones from England and Wales: chemostratigraphic signals and the early Toarcian anoxic event. *Sedimentology* **44**, 687–706.
- JENKYN, H. C., GALE, A. S. & CORFIELD, R. M. 1994. Carbon- and oxygen-isotope stratigraphy of the English Chalk and Italian Scaglia and its palaeoclimatic significance. *Geological Magazine* **131**, 1–34.
- JENKYN, H. C., GRÖCKE, D. R. & HESSELBO, S. P. 2001. Nitrogen isotope evidence for water mass denitrification during the Early Toarcian (Jurassic) Oceanic Anoxic Event. *Paleoceanography* **16**, 593–603.
- JENKYN, H. C., JONES, C. E., GRÖCKE, D. R., HESSELBO, S. P. & PARKINSON, D. N. 2002. Chemostratigraphy of the Jurassic System: applications, limitations and implications for palaeoceanography. *Journal of the Geological Society, London* **159**, 351–78.
- JENKYN, H. C., MATTHEWS, A., TSIKOS, H. & EREL, Y. 2007. Nitrate reduction, sulfate reduction, and sedimentary iron isotope evolution during the Cenomanian–Turonian oceanic anoxic event. *Paleoceanography* **22**, PA3208, doi: 10.1029/2006PA001355, pp. 17

- JENKYN, H. C., SARTI, M., MASETTI, D. & HOWARTH, M. K. 1985. Ammonites and stratigraphy of Lower Jurassic black shales and pelagic limestones from the Belluno Trough, Southern Alps, Italy. *Eclogae Geologicae Helveticae* **78**, 299–311.
- KARAKITSIOS, V. 1995. The influence of preexisting structure and halokinesis on organic matter preservations and thrust system evolution in the Ionian Basin, Northwest Greece. *American Association of Petroleum Geologists Bulletin* **79**, 960–80.
- KARAKITSIOS, V., TSIKOS, H., VAN BREUGEL, Y., BAKOPOULOS, I. & KOLETTI, L. 2004. Cretaceous Oceanic Anoxic Events in Western Continental Greece. *Bulletin of the Geological Society of Greece* **36**, 846–55.
- KARAKITSIOS, V., TSIKOS, H., VAN BRUEGEL, Y., KOLETTI, L., SINNINGHE DAMSTÉ, J. S. & JENKYN, H. C. 2007. First evidence for the late Cenomanian Oceanic Anoxic Event (OAE2, or ‘Bonarelli’ event) from the Ionian Zone, western continental Greece. *International Journal of Earth Sciences (Geol. Rundsch)* **96**, 343–52.
- KEMP, D. B., COE, A. L., COHEN, A. S. & SCHWARK, L. 2005. Astronomical pacing of methane release in the Early Jurassic period. *Nature* **437**, 396–9.
- KÜSPERT, W. 1982. Environmental changes during oil shale deposition as deduced from stable isotope ratios. In *Cyclic and Event Stratification* (eds G. Einsele & A. Seilacher), pp. 482–501. Berlin: Springer-Verlag.
- LEFÈVRE, C., CABANIS, B., FERRIÈRE, J., THIEBAULT, F. & PLATEVOET, R. 1993. Mise en évidence d’une dualité dans le volcanisme triasique hellénique: apport de la géochimie des éléments traces. *Comptes Rendus de l’Académie des Sciences, Paris, Série 2* **316**, 1311–18.
- LITTLE, C. T. S. & BENTON, M. J. 1995. Early Jurassic mass extinction: A global long-term event. *Geology* **23**, 495–8.
- LITTLER, K., HESSELBO, S. P. & JENKYN, H. C. 2010. A carbon-isotope perturbation at the Pliensbachian–Toarcian boundary: evidence from the Lias Group, NE England. *Geological Magazine* **147**, 181–92.
- LYBERIS, N., CHOTIN, P. & DOUBINGER, J. 1980. Précisions stratigraphiques sur la série du Pinde (Grèce): la durée de sédimentation des ‘radiolarites’. *Comptes Rendus de l’Académie des Sciences, Paris, série D* **290**, 1513–16.
- MAILLIOT, S., ELM, S., MATTIOLI, E. & PITTET, B. 2007. Calcareous nannofossil assemblages across Pliensbachian/Toarcian boundary at the Peniche section (Ponta do Trovão, Lusitanian Basin). *Ciências da Terra (Lisbon)* **16**, 1–14.
- MAILLIOT, S., MATTIOLI, E., GUÉX, J. & PITTET, B. 2006. The Early Toarcian Anoxic Crisis, a synchronous event in the Western Tethys? An approach by Quantitative Biochronology (Unitary Associations), applied on calcareous nannofossils. *Palaeogeography, Palaeoclimatology, Palaeoecology* **240**, 562–86.
- MATTIOLI, E. & ERBA, E. 1999. Synthesis of calcareous nannofossil events in Tethyan Lower and Middle Jurassic successions. *Rivista Italiana di Paleontologia e Stratigrafia* **105**, 343–76.
- MATTIOLI, E., PITTET, B., BUCEFALO PALLIANI, R., RÖHL, H.-J., SCHMID-RÖHL, A., MORETTINI, E., MORGANS-BELL, H. S. & COHEN, A. S. 2004. Phytoplankton evidence for the timing and correlation of palaeoceanographical changes during the early Toarcian oceanic anoxic event (Early Jurassic). *Journal of the Geological Society, London* **161**, 685–93.
- MATTIOLI, E., PITTET, B., SUAN, G. & MAILLOT, S. 2008. Calcareous nannoplankton changes across the early Toarcian oceanic anoxic event in the western Tethys. *Paleoceanography* **23**, PA3208, doi:10.1029/2007PA001435, pp. 17
- MCARTHUR, J. M., DONOVAN, D. T., THIRLWALL, M. F., FOUKE, B. W. & MATTEY, D. 2000. Strontium isotope profile of the early Toarcian (Jurassic) oceanic anoxic event, the duration of ammonite biozones, and belemnite palaeotemperatures. *Earth and Planetary Science Letters* **179**, 269–85.
- PE-PIPER, G. 1998. The nature of Triassic extension-related magmatism in Greece: evidence from Nd and Pb isotope geochemistry. *Geological Magazine* **135**, 331–48.
- PE-PIPER, G. & HATZIPANAGIOTOU, K. 1993. Ophiolitic rocks of the Kerassies-Milia Belt, continental Greece. *Ophioliti* **18**, 157–69.
- RIGAKIS, N. & KARAKITSIOS, V. 1998. The source rock horizons of the Ionian Basin (NW Greece). *Marine and Petroleum Geology* **15**, 593–617.
- ROBERTSON, A. H. F., CLIFT, P. D., DEGNAN, P. J. & JONES, G. 1991. Palaeogeographic and palaeotectonic evolution of the Eastern Mediterranean Neotethys. *Palaeogeography, Palaeoclimatology, Palaeoecology* **87**, 289–343.
- ROBERTSON, A. H. F. & KARAMATA, S. 1994. The role of subduction-accretion processes in the tectonic evolution of the Mesozoic Tethys in Serbia. *Tectonophysics* **234**, 73–94.
- RÖHL, H.-J., SCHMID-RÖHL, A., OSCHMANN, W., FRIMMEL, A. & SCHWARK, L. 2001. The Posidonia Shale (Lower Toarcian) of SW-Germany: an oxygen-depleted ecosystem controlled by sea level and palaeoclimate. *Palaeogeography, Palaeoclimatology, Palaeoecology* **165**, 27–52.
- ROSALES, I., ROBLES, S. & QUESADA, S. 2004. Elemental and oxygen isotope composition of Early Jurassic belemnites; salinity vs. temperature signals. *Journal of Sedimentary Research* **74**, 342–54.
- SABATINO, N., NERI, R., BELLANCA, A., JENKYN, H. C., BAUDIN, F., PARISI, G. & MASETTI, D. 2009. Carbon-isotope records of the Early Jurassic (Toarcian) oceanic anoxic event from the Valdorbia (Umbria-Marche Apennines) and Monte Mangart (Julian Alps) sections: palaeoceanographic and stratigraphic implications. *Sedimentology* **56**, 1307–28.
- SCHOUTEN, S., VAN KAAM-PETERS, H. M. E., RIJPSMA, W. I. C., SCHOELL, M. & SINNINGHE DAMSTÉ, J. S. 2000. Effects of an oceanic anoxic event on the stable carbon isotopic composition of Early Toarcian carbon. *American Journal of Science* **300**, 1–22.
- SUAN, G., MATTIOLI, E., PITTET, B., MAILLIOT, S. & LÉCUYER, C. 2008. Evidence for major environmental perturbation prior to and during the Toarcian (Early Jurassic) oceanic anoxic event from the Lusitanian Basin, Portugal. *Paleoceanography* **23**, PA1202, doi: 10.1029/2007PA001459, pp. 14
- SVENSEN, H., PLANKE, S., CHEVALLIER, L., MALTHERSØRENSEN, A. CORFU, F. & JAMTVEIT, B. 2007. Hydrothermal venting of greenhouse gases triggering Early Jurassic global warming. *Earth and Planetary Science Letters* **256**, 554–66.
- TREMOLADA, F., VAN DE SCHOOTBRUGGE, B. & ERBA, E. 2005. Early Jurassic schizosphaerellid

- 898 crisis in Cantabria, Spain: Implications for calci- 917  
899 fication rates and phytoplankton evolution across 918  
900 the Toarcian oceanic anoxic event, *Paleocean-* 919  
901 *ography* **20**, PA2011, doi:10.1029/2004PA001120, 920  
902 pp. 11. 921
- VAN BRUEGEL, Y., BAAS, M., SCHOUTEN, S., MATTI- 922  
903 OLI, E. & SINNINGHE DAMSTÉ, J. S. 2006. Isoreni- 923  
904 eratane record in black shales from the Paris Basin, 924  
905 France: Constrains on recycling of respired CO<sub>2</sub> 925  
906 as a mechanism for negative carbon isotope shifts 926  
907 during the Toarcian oceanic anoxic event. *Paleocean-* 927  
908 *ography* **21**, PA4220, doi: 10.1029/2006PA001305, 928  
909 pp. 8. 929
- VAN DE SCHOOTBRUGGE, B., MCARTHUR, J. M., BAILEY, 930  
911 T. R., ROSENTHAL, Y., WRIGHT, J. D. & MILLER, 931  
912 G. K. 2005. Toarcian oceanic anoxic event: An 932  
913 assessment of global causes using belemnite C iso- 933  
914 tope records. *Paleoceanography* **20**, PA3008, doi: 934  
915 10.1029/2004PA001102, pp. 12 935
- WIGNALL, P. B., MCARTHUR, J. M., LITTLE, C. T. S. & 917  
918 HALLAM, A. 2006. Methane release in the Early Jurassic 918  
919 period. *Nature* **441**, E5, doi: 10.1038/nature04905, 919  
920 pp. 1 920
- WIGNALL, P. B., NEWTON, R. J. & LITTLE, C. T. S. 2005. 921  
922 The timing of paleoenvironmental change and cause- 922  
923 and-effect relationships during the Early Jurassic mass 923  
924 extinction in Europe. *American Journal of Science* **305**, 924  
925 1014–32. 925
- WOODFINE, R. G., JENKYN, H. C., SARTI, M., BARONCINI, 926  
927 F. & VIOLANTE, C. 2008. The response of two 927  
928 Tethyan carbonate platforms to the early Toarcian 928  
929 (Jurassic) oceanic anoxic event: environmental change 929  
930 and differential subsidence. *Sedimentology* **55**, 1011– 930  
931 28. 931
- WOOLER, D. A., SMITH, A. G. & WHITE, N. 1992. Measuring 932  
933 lithospheric stretching on Tethyan passive margins. 933  
934 *Journal of the Geological Society, London* **149**, 517– 934  
935 32. 935